2011

Stability and electronic structure of bilayer graphone

J. Zhou
Center for Applied Physics and Technology

Q. Wang
Virginia Commonwealth University

Q. Sun
Virginia Commonwealth University, Center for Applied Physics and Technology, sunqiang@pku.edu.cn

Puru Jena
Virginia Commonwealth University, pjena@vcu.edu

Stability and electronic structure of bilayer graphone

J. Zhou,[1] Q. Wang,[2] Q. Sun,[1,2,a)] and P. Jena[2]

[1]*Department of Advanced Materials and Nanotechnology, Center for Applied Physics and Technology, Peking University, Beijing 100871, People's Republic of China*
[2]*Department of Physics, Virginia Commonwealth University, Richmond, Virginia 23284, USA*

Stability, reconstruction, and electronic structure of a bilayer graphone have been studied, where the most stable configuration undergoes a (1×2) surface reconstruction. An energy barrier of 1.83 eV separates this structure from the nonbonded state. The stability of the reconstructed bilayer at room temperature is confirmed by both frequency calculation and molecular dynamics simulation. Unlike the graphone sheet, the bilayer graphone is nonmagnetic but remains metallic due to the existence of delocalized π orbital on the zigzag sp^2 carbon chains, which are stable against Peierls instability. The metallicity is also stable under gate external electric field. © 2011 American Institute of Physics. [doi:10.1063/1.3555431]

Recently, graphene[1] has emerged as a classic example where dimensionality plays an important role in many of its new properties.[2] Many strategies of modulating the electronic and magnetic properties of graphene have been proposed and carried out.[3–5] For example, fully hydrogenated graphene (graphane) has been predicted[3] to be a nonmagnetic semiconductor with a band gap of 4.5 eV, and was synthesized[4] by exposing graphene in H plasma environment. It was also predicted[5] that a semihydrogenated graphene sheet where only half of the C atoms on one side of graphene are bonded to hydrogen, the material termed as graphone can become ferromagnetic at room temperature. This is due to partial breaking of π bond of pristine graphene and the formation of alternative $sp^2 - sp^3 - sp^2 - \cdots C$ hybridization pattern. The graphone sheet can be synthesized by supporting graphene first on a substrate and then hydrogenation, as demonstrated in the recent experiment.[6] Since both graphene and graphone show remarkable properties, it is interesting to investigate the property and structure when they bind together.

Note that in the absence of H, two pristine graphene sheets cannot be bonded together due to the weak van der Waals interaction. However, since unsaturated C sites in the graphone sheet are reactive because of unpaired electrons, a graphene sheet can bind to graphone and the system can be viewed as semihydrogenated bilayer graphene (we refer to it as BL-graphone). One simple model of BL-graphone was established by directly bonding graphone and graphene sheets in Bernal *AB* pattern (we refer to it as AB-configuration).[7] Here half of the C atoms in graphene side bonded with graphone (sp^3 hybridization) leaving the other C atoms unsaturated (sp^2 hybridization) analogous to that in graphone. However, this $\cdots - sp^2 - sp^3 - sp^2 - \cdots$ alternative C structure is not the most stable configuration. Using first principles calculations we have systematically studied the stability, geometric and electronic structure of BL-graphone. Unlike a single layer graphone, we find that the unhydrogenated side of this BL-graphone (graphene supported graphone) undergoes a (1×2) surface reconstruction. This consists of parallel sp^2 hybridized zigzag quasilinear C

chains with p_z electrons forming delocalized π orbitals along the chain, making the system metallic but nonmagnetic.

Our first principles calculations are based on spin polarized density functional theory with generalized gradient approximation[8] of exchange correlation potential implemented in DMOL3 package.[9] The exchange correlation functional chosen here is due to Perdew, Burke, and Ernzerhof. Periodic boundary condition is used to simulate two-dimensional infinite structure, and the rhombus supercell contains fourfold unit cells of bilayer in order to investigate the magnetism and geometric relaxation of the system. Vacuum space of ~ 16 Å between two images along the z direction is applied in order to avoid interactions between them. $6 \times 6 \times 1$ Monkhorst–Pack special k-point mesh[10] is used to represent the reciprocal space. The convergence of energy in self consistent field (SCF) calculations is set as 1×10^{-6} hartree. Geometric relaxations are performed without symmetric constraints and the convergence of maximum force and displacement is set as 0.02 eV/Å and 0.005 Å, respectively. Transition state (TS) calculation of reaction pathway is based on the linear and quadratic synchronous transit searching method. Besides rhombus supercell, we also used a rectangular supercell to calculate the geometric optimization and electronic structure. The results remained the same. Hence we will only discuss the results based on the rhombus supercell. Different exchange correlation functional such as BLYP (Refs. 11 and 12) are also used to verify our conclusions. Geometric and electronic calculations are also repeated using the VASP code[13,14] with both supercells, and we obtained similar results.
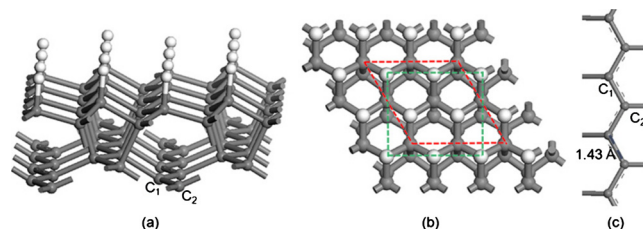

FIG. 1. (Color online) (a) Side view and (b) top view of BL-graphone. The rhombus and rectangle denote two simulation supercells. (c) Zigzag C-chain with sp^2 bonding.
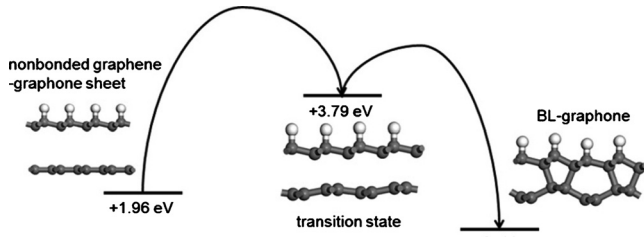
a)Electronic mail: sunqiang@pku.edu.cn.

FIG. 2. Illustration of reaction pathway from a nonbonded graphene-graphone to a bonded BL-graphone.

FIG. 3. Fluctuations of temperature and total energy of BL-graphone as a function of time step obtained from MD simulation.

The bonded BL-graphone can be achieved by applying external vertical pressure to graphone resting on a graphene sheet. We find the unhydrogenated graphene can to undergo a (1×2) reconstruction with only half of C atoms bonded with the unsaturated C atoms in graphone while the remaining C atoms (atoms C_1 and C_2 labeled in Fig. 1) form a zigzag chainlike structure. The bond length between atoms C_1 and C_2 is calculated to be uniformly 1.43 Å which is intermediate between C–C single and double bonds, forming a periodic aromatic chain. Note that this length is quite similar to that of graphene, namely, 1.42 Å. Thus, we can infer that C_1 and C_2 are both sp^2 hybridized and the remaining p_z electrons form a big π orbital along the chain. This can be denoted as $(\sigma + \pi)$ bond as shown in Fig. 1(c). Other C atoms are all sp^3 hybridized and the bond lengths between them are larger than 1.50 Å which represent C–C single bonds. Energetically, this reconstructed configuration is more favorable than the nonbonded graphene–graphone bilayer (interacting only via van der Waals forces) and unreconstructed AB-configuration by 1.96 eV and 2.81 eV, respectively. Along the reaction pathway from a nonbonded configuration to a bonded one there is an energy barrier of 1.83 eV/supercell (see Fig. 2). The reaction is exothermic while the formation of AB-configuration is endothermic. We find that the distance between graphene and graphone sheet decreases about 1.33 Å for TS with respect to initial nonbonded bilayer. Thus, we can estimate that such reaction requires ~10.22 GPa pressure so as to overcome the transition barrier. Such pressure can be achieved in experiments and the graphite is stable under pressure.[15] In addition, we note that the configuration
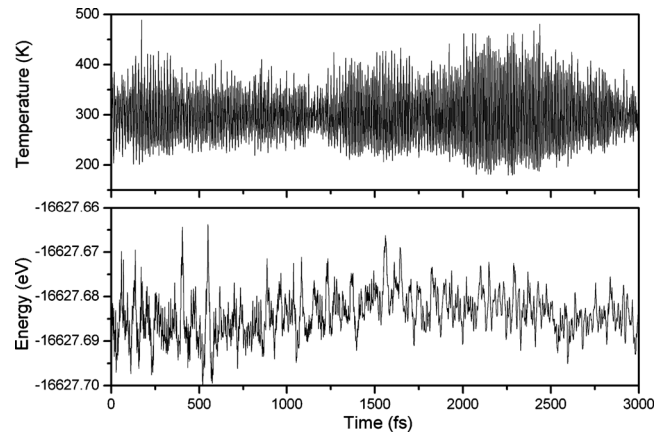
of carbon atoms in BL-graphone is very similar to that of bulk *M*-carbon, which has been achieved in experiment[15] and examined in theoretical work,[16] where the transition happens at pressure of ~14 GPa, comparable with our result.

To further confirm the stability of BL-graphone, we performed vibrational frequency calculation using finite difference method by displacing each atom slightly in three directions. No imaginary frequencies are found and the lowest frequency is calculated to be 350.0 cm^{-1}, which shows that the structure is dynamically stable. Thermal stability of BL-graphone is considered by performing molecular dynamics (MD) simulations with constant temperature of 300 K using Nose–Hoover heat bath scheme. We find that after 3000 time steps with the time step of 1 fs the system distorted slightly, but can be reoptimized to previous static structure. In Fig. 3 we plot the fluctuations of the simulating temperature and the total energy of the system. These results demonstrate that the bilayer structure is dynamically stable and can be maintained at room temperature.

To explore the electronic and magnetic properties of BL-graphone, band structure and partial density of states (PDOS) are calculated (Fig. 4). We find that this BL-graphone is nonmagnetic. The difference in magnetic behavior between AB-model (or isolated graphone) and our reconstructed bilayer is
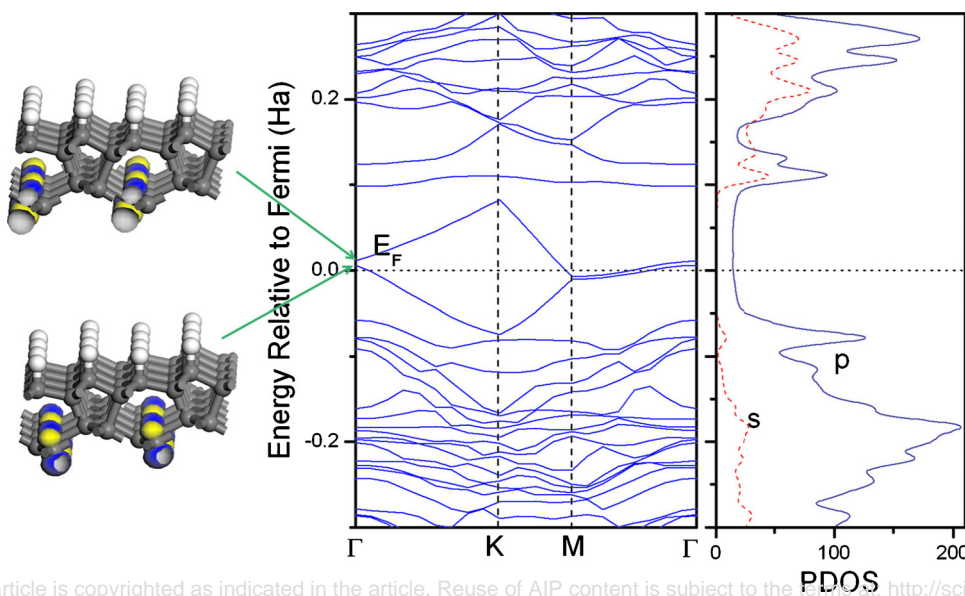

FIG. 4. (Color online) Band structure and the corresponding PDOS plot of BL-graphone. Left panel: wave function of metallic bands at Γ point.

attributed to the different environments of sp^2 hybridized C atoms. Ferromagnetism observed in previous model comes from the broken π orbital and unsaturated sp^2 hybridized C while in the latter model the π orbitals from C_1 and C_2 are intact. To our surprise, two bands at the Γ point in the band structure plot are nearly degenerate and go across the Fermi level indicating metallic property of BL-graphone. Comparing with the metallicity of pristine graphene sheet, the metallic behavior of BL-graphone is not due to single Dirac point. We calculated wave functions at the Γ point, which demonstrates that two metallic bands are contributed by the p_z electrons (big π orbital along C_1–C_2 chain) of C_1 and C_2 atoms, respectively. Consequently, PDOS also shows that p orbital crosses the Fermi level. In order to examine the electron behavior of C_1–C_2 chain, we calculate electron localization function (ELF) and find that the electrons are well delocalized on C_1–C_2 chain thus contributing to metallic conductivity.

Since the metallic behavior is due to the existence of quasilinear C–C chains, readers may wonder whether the structure exhibits Peierls instability with dimerization of C_1 and C_2 atoms, forming alternative single and double C–C bonds instead of $(\sigma+\pi)$ bonds. If that happens, the metallic state may not be stable and the system would change to a semiconducting state. To explore this, we tried many possible dimer geometries as starting structures and performed geometric optimization using both the DMOL3 and VASP code and using rhombus as well as rectangular supercells. In addition, we have also doubled the cell lattice along the x and y directions in order to reduce the periodicity-induced constraints. After relaxation most of the structures changed back to nondimerized structure as stated before. Only one dimerized structure was found with C_1–C_2 bond length alternating between 1.41 and 1.47 Å. However, vibrational frequency analysis shows that this structure has many imaginary frequencies (with the largest one being −488.5 cm^{-1}). Therefore, we conclude that the structure proposed here will not possess Peierls instability and is indeed a local minimum on the potential energy surface. This result is also consistent with the previous study of one-dimensional carbon atomic chain on C (111).[17]

It has been shown that external gate E-field can tune the band gap of semihydrogenated bilayer graphene in AB-configuration because of electron redistribution.[7] So we also consider the effect of E-field on this metallic BL-graphone. Sawtooth-like E-field can be applied in DMOL3 package by including $-e\Phi$ term in the Hamiltonian of the system. Under intermediate E-field ($\sim$0.5 V/Å) we find that the BL-graphone sheet still maintains its metallic property with no obvious variation in the band structure. This can be easily understood; although the electron will redistribute under E-field, the structure of BL-graphone still remains intact and the big π orbital is maintained. Note that for pristine metallic bilayer graphene, the band gap opens under less than 0.1 V/Å.[18] Therefore, we show that the metallicity of BL-graphone is strong as compared to bilayer graphene sheets.

In conclusion, we have studied the geometric structure and electronic property of BL-graphone. Main results are summarized as follows: (1) The bonded bilayer undergoes (1×2) reconstruction. The binding between graphene and graphone sheet is exothermic and requires 1.83 eV/supercell to overcome the energy barrier. (2) The BL-graphone is energetically and dynamically stable as verified by vibrational frequency analysis and MD simulation. (3) Unlike a single layer graphone sheet, the BL-graphone is nonmagnetic, owing to the complete π orbital on chainlike C caused by surface reconstruction. (4) The π orbital of carbon chains makes the system metallic but directional in conductivity, and possesses no Peierls instability. (5) The metallic property is stable under external gate E-field. Currently there are several kinds of metallic C-based nanomaterials: carbon nanotubes, pristine graphene and zigzag graphene nanoribbons, 5-, 8-ring frameworks,[19–21] and 4-, 6-, 8- ring frameworks.[22] Our metallic BL-graphone will enrich this family. Moreover, the strong and directional metallicity in the BL-graphone may have potential application in atomic level electrode for nanocircuits or device elements.

[1] K. S. Novoselov, A. K. Geim, S. V. Morozov, D. Jiang, Y. Zhang, S. V. Dubonos, I. V. Grigorieva, and A. A. Filrsov, Science **306**, 666 (2004).
[2] A. K. Geim, Science **324**, 1530 (2009).
[3] J. O. Sofo, A. S. Chaudhari, and G. D. Barber, Phys. Rev. B **75**, 153401 (2007).
[4] D. C. Elias, R. R. Nair, T. M. G. Mohiuddin, S. V. Morozov, P. Blake, M. P. Halsall, A. C. Ferrari, D. W. Boukhvalov, M. I. Katsnelson, A. K. Geim, and K. S. Novoselov, Science **323**, 610 (2009).
[5] J. Zhou, Q. Wang, Q. Sun, X. S. Chen, Y. Kawazoe, and P. Jena, Nano Lett. **9**, 3867 (2009).
[6] R. Balog, B. Jørgensen, L. Nilsson, M. Andersen, E. Rienks, M. Bianchi, M. Fanetti, E. Lægsgaard, A. Baraldi, S. Lizzit, Z. Sljivancanin, F. Besenbacher, B. Hammer, T. G. Pedersen, P. Hofmann, and L. Hornekær, Nature Mater. **9**, 315 (2010).
[7] D. K. Samarakoon and X.-Q. Wang, ACS Nano **4**, 4126 (2010).
[8] J. P. Perdew, K. Burke, and M. Ernzerhof, Phys. Rev. Lett. **77**, 3865 (1996).
[9] B. Delley, J. Chem. Phys. **92**, 508 (1990); **113**, 7756 (2000)
[10] H. J. Monkhorst and J. D. Pack, Phys. Rev. B **13**, 5188 (1976).
[11] A. D. Becke, J. Chem. Phys. **98**, 5648 (1993).
[12] C. Lee, W. Yang, and R. G. Parr, Phys. Rev. B **37**, 785 (1988).
[13] G. Kresse and J. Furthmuller, Phys. Rev. B **54**, 11169 (1996).
[14] G. Kresse and J. Joubert, Phys. Rev. B **59**, 1758 (1999).
[15] W. L. Mao, H.-K. Mao, P. J. Eng, T. P. Trainor, M. Newville, C.-C. Kao, D. L. Heinz, J. Shu, Y. Meng, and R. J. Hemley, Science **302**, 425 (2003).
[16] Q. Li, Y. Ma, A. R. Oganov, H. Wang, H. Wang, Y. Xu, T. Cui, H.-K. Mao, and G. Zou, Phys. Rev. Lett. **102**, 175506 (2009).
[17] H.-J. Kim, S. Oh, K.-S. Kim, Z. Zhang, and J.-H. Cho, Phys. Rev. B **82**, 041401 (2010).
[18] E. V. Castro, K. S. Novoselov, S. V. Morozov, N. M. R. Peres, J. M. B. Lopes dos Santos, J. Nilsson, F. Guinea, A. K. Geim, and A. H. Castro Neto, Phys. Rev. Lett. **99**, 216802 (2007).
[19] V. H. Crespi, L. X. Benedict, M. L. Cohen, and S. G. Louie, Phys. Rev. B **53**, R13303 (1996).
[20] H. Terrones, M. Terrones, E. Hernández, N. Grobert, J.-C. Charlier, and P. M. Ajayan, Phys. Rev. Lett. **84**, 1716 (2000).
[21] J. Lahiri, Y. Lin, P. Bozkurt, I. I. Oleyink, and M. Batzill, Nat. Nanotechnol. **5**, 326 (2010).
[22] M. A. Hudspeth, B. W. Whitman, V. Barone, and J. E. Peralta, ACS Nano **4**, 4565 (2010).